

# Exploratory Visualization of Animal Kinematics Using Instantaneous Helical Axes

D. F. Keefe<sup>1</sup>, T. M. O'Brien<sup>1</sup>, D. B. Baier<sup>2</sup>, S. M. Gatesy<sup>2</sup>, E. L. Brainerd<sup>2</sup>, D. H. Laidlaw<sup>1</sup>

<sup>1</sup>Brown University Department of Computer Science

<sup>2</sup>Brown University Department of Ecology and Evolutionary Biology

---

## Abstract

*We present novel visual and interactive techniques for exploratory visualization of animal kinematics using instantaneous helical axes (IHAs). The helical axis has been used in orthopedics, biomechanics, and structural mechanics as a construct for describing rigid body motion. Within biomechanics, recent imaging advances have made possible accurate high-speed measurements of individual bone positions and orientations during experiments. From this high-speed data, instantaneous helical axes of motion may be calculated. We address questions of effective interactive, exploratory visualization of this high-speed 3D motion data. A 3D glyph that encodes all parameters of the IHA in visual form is presented. Interactive controls are used to examine the change in the IHA over time and relate the IHA to anatomical features of interest selected by a user. The techniques developed are applied to a stereoscopic, interactive visualization of the mechanics of pig mastication and assessed by a team of evolutionary biologists who found interactive IHA-based analysis a useful addition to more traditional motion analysis techniques.*

Categories and Subject Descriptors (according to ACM CCS): I.3.7 [Computer Graphics]: Three-Dimensional Graphics and Realism – Animation I.3.7 [Computer Graphics]: Three-Dimensional Graphics and Realism – Virtual reality

---

## 1. Introduction

Analysis of 3D motion plays an important role in many scientific processes. In biomechanics, analysis of the rigid body motion of bones is integral in the treatment of disease and injury [Win90] and in the study of animal behavior and evolution [Bie03]. Visual analysis tools have a long history of use in these fields, dating back to the pioneering work of Maray, Muybridge, and their contemporaries [Bra94]. Imaging capabilities have improved considerably, and scientists now benefit from a new ability to collect accurate high-speed motion data of internal anatomical structures, such as bones, during motion experiments [YSAT01]. In this paper, we examine novel visual and interactive techniques for analysis of this 3D kinematic data.

As a rigid body, such as a bone, moves through space, it undergoes both translation and rotation. This movement may be represented mathematically by several alternative strategies, including a 4x4 transformation matrix, a combination

of rotation angles and translation vectors, or the parameters of a “screw” motion (a translation along and rotation about an axis in space). In this paper, we explore interactive visualization and analysis techniques using screw axes, known more commonly within the biomechanics community as helical axes.

Helical axis representations exhibit several properties that make them advantageous for the study of motion. First, they permit a description of rigid body motion without requiring an arbitrarily chosen reference frame. In contrast, alternative strategies, such as rotation angles (Euler or Cardan) combined with  $X, Y, Z$  translation values, require reporting data relative to a locally defined reference frame. In experimental contexts, care must be taken to define this frame consistently across subjects and in a way that facilitates analysis of the most important components of the data. To ease this burden, several conventions have been defined, for example, Denavit-Hartenberg (DH) notation [Ang02], and the joint ro-

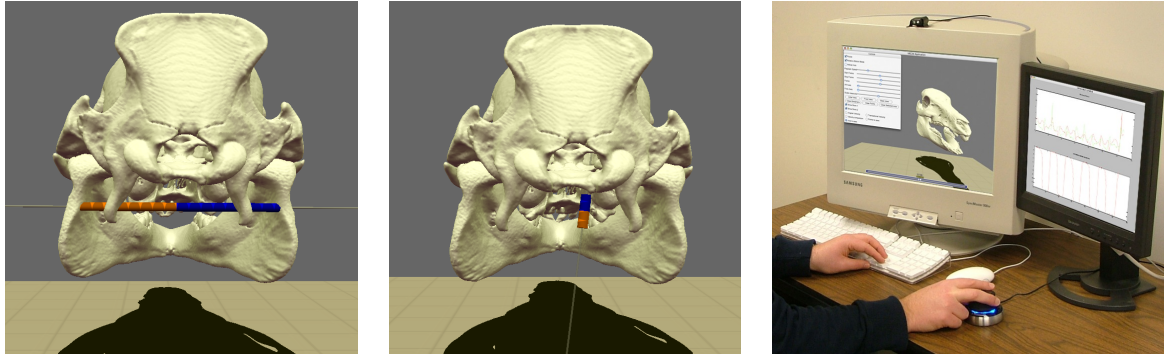


**Figure 1:** Visualization of the motion of a pig's mandible while chewing. Left and middle: View from behind the pig's head during the opening phase (left) and food grinding phase (middle). The IHA displayed describes the mandible's motion at each instant shown. Right: The visualization environment including a stereoscopic display on the left, linked 2D data plots on the right, and controlled via a combination of the mouse, keyboard, and a 6-DOF SpaceNavigator.

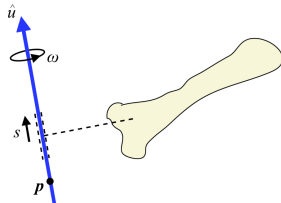


**Figure 2:** Instantaneous helical axis (IHA) for a moving, rigid body.

tation convention (JRC) [Zat98]. Both of these work well in specific applications. DH notation is useful for describing motion of complex, multi-link mechanisms in robotics. Useful in biomechanical analysis, the JRC system defines spatial reference axes with respect to proximal and distal body segments, making analysis more direct for some joints, the knee for example. Our intent is not to replace these useful strategies, but rather to explore more thoroughly the cases where alternative representations may compliment existing approaches, for example, in analysis of bones with multiple complex articulations, such as the mandible.

Another advantageous property of helical axes is the direct visual interpretation that viewing the axis together with an anatomical reference sometimes provides. For example, in Figure 1 (left), a helical axis for one time-step during the opening phase of a pig's chewing motion is displayed together with correctly posed 3D bone geometries. Notice the horizontal positioning of the helical axis, indicating immediately that the rotational component of the motion at this point functions to open the jaw. Also, notice the intersection of the axis with the geometry of the mandible. Rather than passing through the temporomandibular joint (TMJ) itself, as we would expect of a simple hinge joint (rotation only), the axis

**Table 1:** Parameters of the IHA.

$\hat{u}$	=	unit direction of IHA
$\omega$	=	magnitude of angular velocity
$s$	=	magnitude of sliding velocity along IHA
$\mathbf{p}$	=	a point coincident with IHA

intersects the mandible at a lower point, providing an immediate indication to the viewer of the "sliding" that happens within the TMJ as the mandible protrudes forward when the jaw opens. The utility of direct visual interpretations of this nature, evident even within a still image, have motivated our investigation of animated, interactive, and stereoscopic visualizations using helical axes.

Our contributions are in three areas. First, we present an exploration of the design space of visual elements that may be used to display all parameters of the IHA within an animated virtual reality presentation. Second, we present interactive strategies for relating IHA parameters to the anatomy, with output in linked 3D and 2D data displays. Third, we present details and feedback from an application in visualization of mastication in pigs. We begin with a discussion of related work before presenting our approach and the resulting application.

## 2. Related Work

The helical axis has application in many fields, from structural mechanics [Som92] to 3D modeling in computer graphics [LKG\*03]. Most closely related to our work are applications in biomechanics, which have included study of the human carpus [CCM\*05], finger [VCR98], arm [LMM00], neck [WLOF94], and jaw [GAAP97, GFP00]. Use of visualization in these contexts is limited to relatively simple views of the axis and the ruled surface that is swept out as

it advances through space during a motion sequence. This is sometimes coupled with statistical analysis of helical axis parameters aimed to address specific hypotheses.

Our work builds upon previous contextualized 3D visualizations of helical axes [VCR98] by adding more time-lapsed views, visual encodings for IHA parameters, and interactivity. We also extend previous helical-axis-based approaches by utilizing high-speed motion data (collected at 250 Hz). Our new ability to collect data at this speed allows for robust estimation of *instantaneous* helical axes (IHAs).

Calculation of instantaneous rather than finite helical axes is governed largely by limitations and availability of appropriate motion sensing technologies. Most previous work has calculated helical axis parameters from finitely-separated poses of bones, either sampled at much slower rates than possible today, or sampled coarsely via placing the body in predetermined poses during an experiment as controlled by a jig. Woltring and colleagues explore the use of optical tracking technology with a capture rate of up to 5 Hz for diagnosis of whiplash based on neck kinematics [WLOF94]. We visualize data from a new biplane fluoroscopy system, similar to that used for analysis of skeletal kinematics in the human knee [YSAT01]. With this system, six degree-of-freedom motion tracking information may be obtained for individual bones at more than 250 Hz. As these new technologies become more prevalent, data appropriate for robust calculation of IHAs will become increasingly available. Thus, we expect interactive strategies for exploring this data to be of great utility in the future.

For clinical application and functional descriptions of joints, it is often important to characterize the helical axis parameters via statistical measures that may be related to the anatomy. Several examples exist within the literature. Common procedures include projecting the axis direction onto planes defined by anatomical landmarks, upon which 2D angle measurements may be made [CCM\*05, GAAP97]. Distance measurements can also be useful. For example, the distance from a joint center to the closest point along the helical axis may be examined over the course of a motion sequence [GAAP97, GFP00]. These connections to anatomical structure are critical for addressing many scientific hypotheses. Our work makes it possible to interactively query the relationship between axis parameters and user-selected features within the surrounding anatomical context and view results in coordinated 2D and 3D displays.

### 3. Introduction to Application to Pig Mastication

In collaboration with a research group of evolutionary biologists, we have been examining kinematic data from several animal species. Examples used to describe our methods come from one project from this collaboration, exploration of the mechanics of pig mastication. A brief description of this data follows.

The motion data driving the visualization come from a biplane fluoroscopy system similar to that described by You et al. [YSAT01]. High-speed (250 Hz) X-Ray movies are captured from two near-orthogonal angles. 3D reconstruction software is used to derive 3D positional information from the X-Ray imagery for radio-dense markers implanted within the bones of interest. When registered with CT scans, the 3D marker data may be used to drive animations of 3D bone geometries extracted from the CT scan. This is the source of the anatomical data in our examples. Helical axis parameters are computed from the 3D marker coordinates as described below.

## 4. Exploratory IHA Visualization

This section describes interactive and visual tools for IHA visualization within the stereoscopic desktop viewing environment pictured in Figure 1 (right). We begin by reviewing the method for calculating IHA parameters from motion data that we have adopted for our work.

### 4.1. Calculating IHAs from Marker-Based Motion Data

To compute the IHA parameters given in Table 1, we follow the framework given in [SB90, Som92]. For any point  $\mathbf{x}$  on a rigid-body in motion, its total velocity  $\vec{v}$  can be defined as a rotation about and translation along a single axis, the IHA. More specifically, given a point  $\mathbf{p}$  coincident with the IHA and the unit length IHA direction vector  $\hat{u}$ ,  $\vec{v}$  may be defined as the sum of the cross product of the angular velocity vector,  $\vec{\omega} = \omega\hat{u}$ , with the location of  $\mathbf{x}$  relative to  $\mathbf{p}$ , plus a sliding velocity component,  $\vec{s} = s\hat{u}$ . This relationship is captured in Equation 1, based in a right-handed Cartesian coordinate system.

$$\vec{v} = \vec{s} + \vec{\omega} \times (\mathbf{x} - \mathbf{p}) \quad (1)$$

Three IHA parameters are unknown in Equation 1. Following the approach presented in [SB90, Som92], we solve for these in a least-squares sense given the  $m$  marker positions recorded at each frame of the data. This procedure involves minimizing the sum of squares of velocity residuals, as given in Equation 2, with respect to the three IHA parameters.

$$R = \frac{1}{m} \sum_1^m (\vec{v}_i - \vec{s} - \vec{\omega} \times (\vec{x}_i - \mathbf{p}))^T (\vec{v}_i - \vec{s} - \vec{\omega} \times (\vec{x}_i - \mathbf{p})) \quad (2)$$

A Lagrange multiplier technique is applied to enforce rigid body constraints. For more complete details, see [SB90, Som92].

In our application, the marker positions are sampled at 250 Hz. A low-pass filter is applied to the resulting time series data for each marker to attenuate high-frequency noise. A finite differencing approach using a sliding window of  $\pm 0.05$  seconds about each frame is used to compute marker velocities for use within the IHA computations.

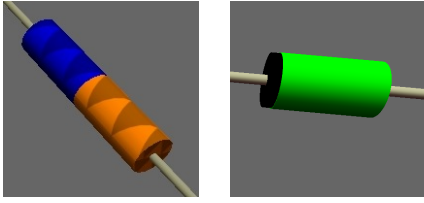


**Figure 3:** Visual encodings for IHA parameters. Left: angular velocity. Right: sliding velocity.

## 4.2. Visualizing IHA Parameters

The parameters of the IHAs calculated from motion data are mapped to visual form as described in the following sections. These mappings can be viewed in isolation in individual inspection modes, or in combination as described in Section 4.4.1.

### 4.2.1. Position and Orientation

The IHA is displayed as an oriented line segment drawn relative to the anatomical data (bones) using a gray cylinder as seen in Figures 1 and 3. The cylinder is oriented to align with the direction  $\hat{u}$  of the IHA. The gray cylinder is made long enough to intersect the bone geometries. These intersection points are clearly seen during stereo viewing and provide visual cues for understanding the orientation of the axis relative to the anatomy.

### 4.2.2. Angular Velocity

The angular velocity  $\omega$  is represented as seen in Figure 3 (left). A half blue, half orange cylinder is drawn on top of the gray one. The length varies linearly with  $\omega$ . A gain factor for this mapping is adjustable by the user and set interactively to tune the display to the particular question under investigation. The direction of rotation is doubly coded on the axis. The blue and orange colors mark sides of the axis. For cyclic animations, this coding scheme makes direction reversals immediately obvious. For example, during jaw opening and closing observed from a posterior view, we see blue on the right for the opening phase and blue on the left for the closing phase.

An arrow texture applied to the cylinder also encodes this directional information. The texture functions in several ways. First, during static viewing the arrows on the texture are useful to indicate the direction of rotation. Second, the visual cue provided by the texture is likely to aid perception of shape and orientation when displayed in a virtual environment [IFP97]. Third, the texture pattern repeats at a fixed spatial interval. Thus, the magnitude of angular velocity may be compared across frames by counting the number of arrows displayed.

Of final note in the design of the angular velocity display is the positioning of the orange/blue cylinder along the axis.

One benefit of the method used to calculate IHA parameters described in section 4.1 is that the point coincident with the axis,  $\mathbf{p}$ , has a geometric meaning with respect to the data. (This is not true of all methods for calculating IHA parameters, as by definition,  $\mathbf{p}$  is only required to be coincident with the axis.) In our implementation,  $\mathbf{p}$  lies along the shortest path from the axis to the centroid of the markers used to calculate the IHA, making it a good “center point” for the axis for most situations where marker-based tracking is used. The orange and blue cylinders are drawn to each extend outward from this center point so that the data display remains centered with respect to the reference established by the anatomical context.

### 4.2.3. Sliding Velocity

The sliding velocity  $s$  along the IHA is represented similarly, as seen in Figure 3 (right). A black mark denotes the center point of the axis. A green cylinder of length proportional to  $s$  is drawn from the center point in the direction of sliding. At times when the direction of sliding reverses, the green mark can be seen flipping to the other side of the fixed black mark, calling attention to the reversal. Alternative designs might ease the task of magnitude comparisons by avoiding this flip. Our goal was to highlight direction reversals and facilitate investigation of trends in the data, leaving precise magnitude comparisons to complimentary 2D visualizations and/or post-hoc statistical analysis.

### 4.2.4. Adjusting the Saliency of Directional Cues

One interesting property of IHAs calculated from experimental data is that the estimation of  $\hat{u}$  is generally less robust when  $\omega$  is small. In fact,  $\hat{u}$  is undefined when  $\omega = 0$ . This is an important consideration for the design of animated displays. If a strong visual depiction for the axis is displayed during times of low angular velocity, the result is a visually dominating, fast moving axis, which has the effect of visually highlighting this noisy portion of the data. To avoid this scenario, the orange/blue cylinder decreases length as described above with low values of  $\omega$  and the gray extension of the axis fades to a transparent value to be less apparent in the visual field during periods of low  $\omega$ .

This encoding is similar in spirit to several other continuous geometric representations used in visualization. The varying-length cylinder in our visualization can be thought of as an approximation of an ellipsoid that morphs between a spherical and cigar shape depending upon the magnitude of angular velocity. In this sense, the visual construct is quite similar to strategies based upon morphing geometric representations used for tensor field visualization [EKR\*05, LAd\*98].

## 4.3. Visualizing Variation over Time

Animated views of the IHA and surrounding bones may be produced with the rate of playback and time window of inter-

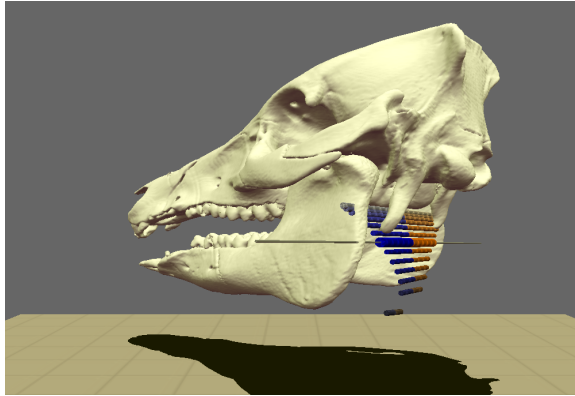


**Figure 4:** View of the IHA extended forward and backward in time. The location of the IHA moves up toward the condyles and angular velocity increases during this closing phase of chewing.

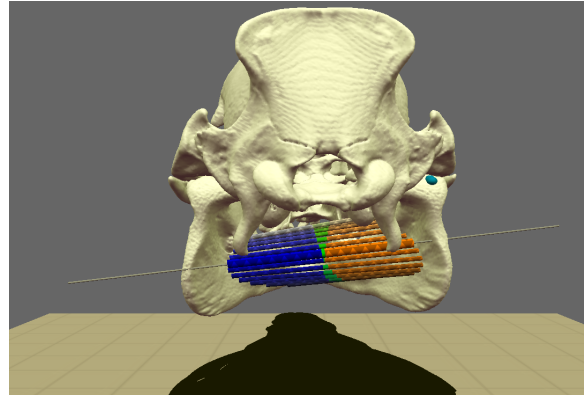


**Figure 5:** After selecting a point of interest on the bone (marked with a small cyan sphere), the relative effect of IHA sliding and rotation parameters with respect to this point is visualized on the axes.

est controlled via on-screen sliders. Additionally, variation in the axis over time may be explored by displaying previous and future axes for each frame of the animation, as seen in Figure 4 and 5. The number to display in each direction is set interactively by the user, allowing for close inspection while stepping through frames of the animation. The effect produces the *sense* of a 3D ruled surface, as seen in Figures 4 and 5.

While arbitrary length judgments in virtual scenes tend to be error prone [NTPT96], the dense arrangement of axes in the time-lapsed view shown in Figure 4 attempts to facilitate relative 3D length judgments of neighboring axes. Interactive controls, using the SpaceNavigator device, allow for reorienting the geometries in space during inspection. Motion and stereo cues from these manipulations are likely to aid in perception of axis orientation and the form swept out by the axes [WF96]. These interactive features are important since perception of 3D form and oriented line segments can, in general, be quite challenging [LBF03,TCN90]. When animated, the time-lapsed display acts as a motion blurring effect operating over the time window specified by the user. Similar motion-blurring and flow-direction highlighting effects have been employed to advantage in fluid flow visualizations [SFL\*04,LKJ\*05].

#### 4.4. Relating to Anatomical Contexts

In many applications, there is a need to relate the helical axis to an anatomical context. We explore methods of establishing a connection to the underlying anatomy using interaction.

##### 4.4.1. Comparing Sliding and Rotation

When working with IHA data, it is important to understand the relative contributions of the two types of motion de-

scribed, rotation captured by the angular velocity  $\omega$  (typical units are radians per second) and translation along the axis captured by the sliding velocity  $s$  (typical units are cm per second). While the helical axis describes the motion of each point on the rigid body as a whole, the relative contributions of rotation and translation vary at each point based on the distance to the axis. Although the two quantities are measured in different units, their relative effects on the movement of a user-specified region of interest may be compared on a common scale.

In the comparison mode of our software, the user selects, via a mouse-controlled ray casting technique, an anatomical feature (point  $\mathbf{q}$ ) on the surface of the bone. Given a time window  $\Delta t$ , the translation due to sliding of this point is

$$d_1 = s\Delta t, \quad (3)$$

while the effective translation of  $\mathbf{q}$  as a result of the rotation around the IHA is

$$d_2 = |R\mathbf{q} - \mathbf{q}|, \quad (4)$$

where  $R$  is the matrix that rotates  $\mathbf{q}$  about the IHA by the angle  $\omega\Delta t$ . By visualizing the values  $d_1$  and  $d_2$ , we are able to compare the contributions of the rotation and sliding components of the IHA to the movement of an anatomical region of interest. An example visual result is seen in Figure 5. In this case, a point of interest, marked with a small cyan sphere, was selected on the mandible. As before, the length of the cylinders surrounding the axis are mapped to sliding and rotation values, but now the two values are in the same units and magnitude comparisons may be made by judging relative lengths and using the scale provided by the arrow texture. Here,  $d_1$  is mapped to the length of the green cylinder and  $d_2$  is mapped to the length of the orange/blue cylinder. We see that the angular velocity described by the IHA con-

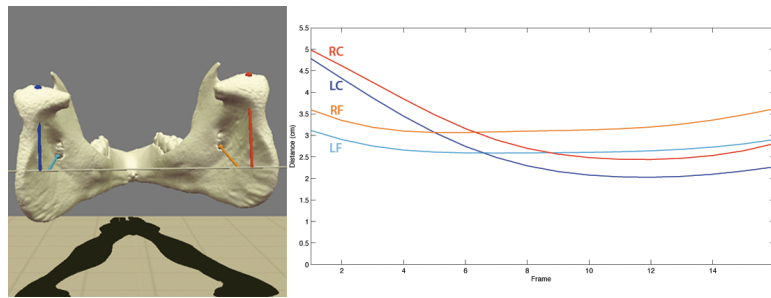


**Figure 6:** The mandibular foramen and condyle on both the left and right sides are selected to produce plots of distance to the IHA during one jaw closing motion. This analysis is relevant to the hypothesis described in section 5.2.

tributes to the motion of the point of interest far more than does the sliding velocity.

#### 4.4.2. Anatomical Context and Axis Position

Points of interest interactively selected by the user may be used to examine the position of the axis in space relative to the anatomy. Figure 6 presents an example in which axis proximity to points at the mandibular foramen and condyles is compared.

#### 4.4.3. Anatomical Context and Axis Orientation

A similar mode shown in Figure 7 plots the dot product of the IHA direction vector  $\hat{u}$  with a vector specified by selecting anatomical features in the display. A reference vector has been created between the two condyles. In the resulting plot, a chewing cycle can be clearly seen. The dot product is close to minus one when the jaw is opening, close to one when closing, and undergoes a transition during a grinding phase.

### 5. User Evaluation

Three evolutionary biologists from our research team participated in a qualitative evaluation of the IHA-based visualizations as applied to the pig mastication data. The lead researcher had previous experience with the visualization, having used a prototype of the system on her desktop for several weeks prior to the session. The other researchers had participated in discussion shaping the development of the visualization tool and were familiar, through these discussions and knowledge of related work in biomechanics, with the notion of helical axes of motion.

#### 5.1. Hypotheses and Discussion

The session began by asking the scientists to review hypotheses they have regarding the study of pig mastication. Our intent was to begin to evaluate which of these candidate hypotheses might lend themselves to evaluation via helical axis techniques and which might not. A few specific

hypotheses were mentioned during this discussion, but the dominant theme expressed by our collaborators was the desire to broadly explore the collected motion data. One researcher explained his data analysis process as starting with a mental image of the mechanics of a joint, likely formed by years of observation and study of similar mechanisms. In examining experimental data, he is looking to see if the data captured match or differ from his mental model. More specific hypotheses are often formed during this broad, exploratory phase.

Initial discussion also focused on the mechanics of the IHA. It was pointed out that the use of helical axes requires a shift in the mindset of many researchers. Joints are typically thought of as being capable of both rotation and translation, but rotation and translation are usually described relative to a reference frame centered in the joint. The helical axis describes rotation and translation in a different manner. In many cases, the helical axis calculated for a motion will not pass directly through a joint. A rotation around such an axis produces a sliding effect in the joint. In most traditional models, this would be characterized as a “translation” relative to a joint-centric coordinate frame. With helical axes this “translation” may actually be described via the rotation parameter of an IHA located outside the joint. Adjusting to analysis in this style requires some thought, but also holds promise. In some cases, for example describing the protrusion of the jaw during chewing, helical axes seem to offer a more direct interpretation of the observed motion.

#### 5.2. Specific Findings

The participants commented specifically on the utility of stereoscopic viewing. The extension of the axis forward and backward in time as seen in Figures 4 and 5 was also singled out as particularly useful for understanding the progression of the motion, as was the comparison of the relative contributions of rotation and sliding to the movement of points of interest on the anatomy. The high temporal resolution of the data with respect to the speed of the motion observed allowed for unique analysis. It was observed that the tran-

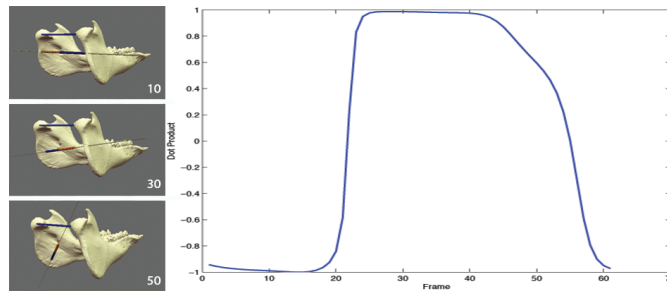


**Figure 7:** The dot product of IHA direction  $\hat{u}$  with a user-selected reference axis. Frame 10: The dot product is near minus one, as the jaw rotates open. Frame 30: The motion has reversed, the dot product is near one, the jaw is closing. Frame 50: The IHA is nearly perpendicular to the reference axis while the mandible undergoes lateral movement to grind the food.

sition from jaw opening to closing was much quicker than from closing to opening. The difference was visible by stepping through frames by hand and counting the time-steps required to transition from one phase to the next as described by the orientation of the IHA. Coarser approximations for the IHA may have missed describing these fast transitioning motions.

A specific hypothesis was investigated using the distance-to-axis tool described in Section 4.4.2 and 2D outputs similar to those reproduced in Figure 6. In humans, it has been proposed that the mandibular axis of rotation may be centered about the mandibular foramen, where the inferior alveolar nerve and artery enter the lower jaw and the vein exits [Mos60]. (For a more contemporary discussion of this hypothesis, see [Che98].) The mandibular foramen can be identified on the mandible model extracted from CT data. It was selected interactively along with points on the condyles, as in Figure 6, to query distances from the points to the IHA during different phases of the motion. Analysis suggests that for some phases of the motion, notably at the beginning of closing phase, the IHA is indeed closer to the mandibular foramen than to the condyles. Later, in preparation for food grinding the IHA tilts and moves closer to the condyles, often passing nearly through one of them as grinding motion moves the teeth away from that condyle in the direction of the other.

### 5.3. Future Directions

Several suggestions were made regarding future additions to the tool that may be useful for biomechanical analysis. One is to trace the intersection of the IHA on the bone models. The suggestion was also made to use IHA-based analysis to segment motions into phases, as in Figure 7, and determine axes of rotation during these phases. If we can then describe the location of average axes of rotation for each phase with reference to the anatomy, we may be able to use these data-derived axes to define more meaningful local reference frames for use in reporting standard measures of motion such as rotation angles.

Several hypotheses presented by the group require comparison of multiple motion sequences. For example, the rate of transition from one phase of chewing to the next may change based on the amount of food in the mouth. Tools facilitating comparison of IHA parameters across multiple motion sequences are likely to be of great value in future analyses of experimental data in biomechanics.

## 6. Conclusions

High-speed 3D motion data from biomechanical experiments capture complex spatial and motion relationships. Stereoscopic views and the ability to step slowly through motion datasets while viewing time-lapsed displays of the IHA are important for capturing this complexity. Also critical for biomechanical analysis using IHAs is relating the axis parameters to the surrounding anatomical context. Three interactive techniques (comparison of sliding and rotation IHA parameters given a feature of interest, plots of distance from the IHA to selected features, and plots of IHA orientation relative to selected features) were useful in this regard and helped with investigating specific hypotheses during the user evaluation.

Analysis using IHAs requires, in some cases, a shift in thinking from traditional approaches to biomechanical analysis. However, IHAs show great potential for forming understandings and providing descriptive accounts of complex motion patterns. The workings of the mandible and temporomandibular joint (TMJ) in pigs provides a case study of a complex motion that is challenging to describe using more traditional rotation and translation parameters. We anticipate the visual and interactive tools presented to be applicable in many other instances as well.

## Acknowledgment

This work was supported in part by the US National Science Foundation (CNS-0427374, DBI-0552051, IOS-0723392, CCR-0086065), and by a grant from the W. M. Keck Foundation.

## References

- [Ang02] ANGELES J.: *Fundamentals of Robotic Mechanical Systems*. Springer-Verlag, 2002.
- [Bie03] BIEWENER A. A.: *Animal Locomotion*. Oxford University Press, 2003.
- [Bra94] BRAUN M.: *Picturing Time: The Work of Etienne-Jules Marey*. University of Chicago Press, 1994.
- [CCM\*05] CRISCO J. J., COBURN J. C., MOORE D. C., AKELMAN E., WEISS A.-P. C., WOLFE S. W.: In vivo radiocarpal kinematics and the dart thrower's motion. *The Journal of Bone and Joint Surgery* 87 (2005), 2729–2740.
- [Che98] CHEN X.: The instantaneous center of rotation during human jaw opening and its significance in interpreting the functional meaning of condylar translation. *American Journal of Physical Anthropology* 106 (1998), 35–46.
- [EKR\*05] ENNIS D. B., KINDLMAN G., RODRIGUEZ I., HELM P. A., MCVEIGH E. R.: Visualization of tensor fields using superquadric glyphs. *Magnetic Resonance in Medicine* 53, 1 (2005), 169–176.
- [GAAP97] GALLO L. M., AIROLDI G. B., AIROLDI R. L., PALLA S.: Description of mandibular finite helical axis pathways in asymptomatic subjects. *Journal of Dental Research* 72, 2 (1997), 704–713.
- [GFP00] GALLO L. M., FUSHIMA K., PALLA S.: Mandibular helical axis pathways during mastication. *Journal of Dental Research* 79, 8 (2000), 1566–1572.
- [IFP97] INTERRANTE V., FUCHS H., PIZER S.: Conveying the 3D shape of smoothly curving transparent surfaces via texture. *IEEE Transactions on Visualization and Computer Graphics* 3, 2 (1997), 98–117.
- [LAd\*98] LAIDLAW D. H., AHRENS E. T., DAVIDKREMER, AVALOS M. J., READHEAD C., JACOBS R. E.: Visualizing diffusion tensor images of the mouse spinal cord. In *Proceedings of IEEE Visualization 1998* (1998), pp. 127–134.
- [LBF03] LIND M., BINGHAM G. P., FORSELL C.: Metric 3d structure in visualizations. In *Proceedings of Information Visualization 2003* (2003), pp. 51–57.
- [LKG\*03] LLAMAS I., KIM B., GARGUS J., ROSSIGNAC J., SHAW C. D.: Twister: a space-warp operator for the two-handed editing of 3D shapes. *ACM Transactions on Graphics* 22, 3 (2003), 663–668.
- [LKJ\*05] LAIDLAW D. H., KIRBY M., JACKSON C., DAVIDSON J. S., MILLER T., DASILVA M., WARREN W., TARR M.: Comparing 2d vector field visualization methods: A user study. *IEEE Transactions on Visualization and Computer Graphics* 11, 1 (2005), 59–70.
- [LMM00] LÁSZLÓ K., M. K. R., MIHÁLY J.: Determination and representation of the helical axis to investigate arbitrary arm movements. *Facta Universitatis - Series: Physical Education* 1, 7 (2000), 31–37.
- [Mos60] MOSS M.: *Disorders of the Temporomandibular Joint*. W.B. Saunders, 1960, ch. Functional Anatomy of the Temporomandibular Joint, pp. 73–88.
- [NTPT96] NORMAN J. F., TODD J. T., PEROTTI V. J., TITTLE J. S.: The visual perception of three-dimensional length. *Journal of Experimental Psychology* 22, 1 (1996), 173–186.
- [SB90] SOMMER H. J., BUCZECK F. L.: Experimental determination of the instant screw axis and angular acceleration axis. In *Proceedings of the 1990 Sixteenth Annual Northeast Bioengineering Conference* (1990), pp. 141–142.
- [SFL\*04] SOBEL J. S., FORSBERG A. S., LAIDLAW D. H., ZELEZNIK R. C., KEEFE D. F., PIVKIN I., KARNIADAKIS G. E., RICHARDSON P., SWARTZ S.: Particle flurries: Synoptic 3D pulsatile flow visualization. *IEEE Computer Graphics and Applications* 24, 2 (March/April 2004), 76–85.
- [Som92] SOMMER III H. J.: Determination of first and second order instant screw parameters from landmark trajectories. *Journal of Mechanical Design* 114 (1992), 274–282.
- [TCN90] TODD J. T., CHEN L., NORMAN J. F.: On the relative salience of euclidean, affine and topological structure for 3d form discrimination. *Perception* 27 (1990), 273–282.
- [VCR98] VAN SINT JAN S. L., CLAPWORTHY G. J., ROOZE M.: Visualization of combined motions in human joints. *IEEE Computer Graphics and Applications* 18, 6 (1998), 10–14.
- [WF96] WARE C., FRANCK G.: Evaluating stereo and motion cues for visualizing information nets in three dimensions. *ACM Transactions on Graphics* 15, 2 (1996), 121–139.
- [Win90] WINTER D. A.: *Biomechanics and Motor Control of Human Movement*. John Wiley and Sons Inc., 1990.
- [WLOF94] WOLTRING H. J., LONG K., OSTERBAUER P. J., FUHR A. W.: Instantaneous helical axis estimation from 3-D video data in neck kinematics for whiplash diagnostics. *Journal of Biomechanics* 27, 12 (1994), 1415–1432.
- [YSAT01] YOU B., SIY P., ANDERST W., TASHMAN S.: In vivo measurement of 3-D skeletal kinematics from sequences of biplane radiographs: Application to knee kinematics. *IEEE Transactions on Medical Imaging* 20, 6 (2001), 514–525.
- [Zat98] ZATSIORSKY V.: *Kinematics of Human Motion*. Human Kinetics Publishers, 1998.